# Geomechanics 93

Strata Mechanics / Numerical Methods / Water Jet Cutting / Mechanical Rock Disintegration

Edited by

**ZIKMUND RAKOWSKI** 

Institute of Geonics of Academy of Sciences of Czech Republic, Ostrava, Czech Republic

**OFFPRINT** 



A.A.BALKEMA/ROTTERDAM/BROOKFIELD/1994

### Modelling of progressive damage evolution in rocks

Zenon Mróz & Maciej Kowalczyk
Institute of Fundamental Technological Research, Warsaw, Poland

ABSTRACT: The ultimate failure of rock is preceded by progression of consecutive damage modes producing very frequently periodic sequence of failure events. The cracking mode is associated with a set of oriented cracks inducing stress redistribution and orthotropic material structure. The crushing and post-buckling modes are associated with subsequent failure of cracked portions thus inducing total collapse.

The evolution of damage zones and the ultimate failure modes are discussed for several cases, namely a) axisymmetric stress state around a borehole with internal pressure inducing progression of damage b) interaction of a rigid punch with rock mass and the variation of penetration force is derived by considering progression of cracking, crushing and shearing modes.

#### 1 INTRODUCTION

The present paper is concerned with the analysis of progressive failure modes in brittle materials, such as rock, ice, concrete, or ceramics. The constitutive models for such materials so far proposed are usually aimed to describe deformation response in the stable regime before reaching the maximal stress and post-critical strain localization, cf. Jaeger and Cook (1976), Derski et al (1989). However, in many technical problems such as rock crushing, cutting or drilling, ice plate interaction with off-shore platforms, etc., there is a need to account for all progressive failure modes with account for post-critical stress-strain response and localized slip or fracture modes. The present paper is addressed to such class of problems and simplified assumptions are introduced in order to generate analytical solutions. Our aim is to demonstrate that evolution of progressive failure modes induces periodicity of failure events with load-displacement curves exhibiting oscillatory character with development and termination of particular modes. The present paper is also aimed to illustrate general properties of solutions of boundary-value problems for brittle-plastic materials, namely periodicity of failure events, interaction of progressive failure and

plastic flow, scale effect, etc. The major failure modes discussed are cracking, crushing, localized shear, buckling and post-buckling of cracked elements.

In Section 2, the analysis of progression of cracked and crushed zones in the axisymmetric case is discussed. In Section 3, the punch penetration problem is analysed in the case of plane strain and plane stress. The load deflection curve is derived and the consecutive failure events are discussed in detail.

## 2 CRACKING AND CRUSHING OF ROCK IN THE VICINITY OF BOREHOLE

Let us first consider an axisymmetric problem of a cylinder acted on by internal pressure and in the limit case of a borehole in an infinite continuum. Assuming the plane strain case, we assume the material to be in elastic, cracking or crushing state, depending on the actual stress state. Figure 1 presents the respective states within the cylinder. The detailed analysis was presented by Kowalczyk and Mróz (1988), following previous studies by Ladanyi (1967) and Helan (1984).

Assume the macrocracks to develop along radial directions and the cracked rock to be regarded

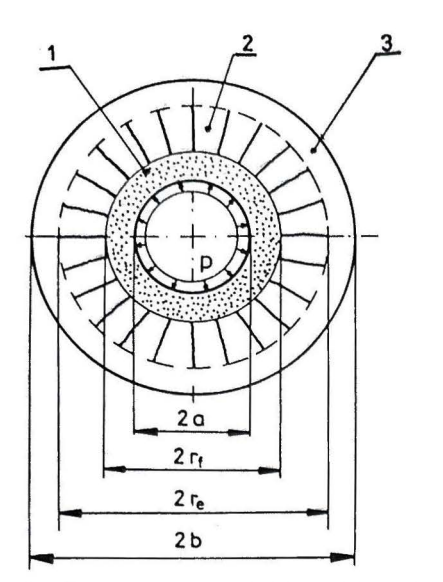


Figure 1: Axisymmetric cylinder with different stress stage zones: 1) crushed 2) cracked 3) elastic

as an orthotropic material of vanishing stiffness moduli in circumferential direction. The total strain components  $\varepsilon_{\tau}$  and  $\varepsilon_{t}$  in radial and circumferential directions are decomposed in the cracked zone as follows

$$\varepsilon_r = \varepsilon_r^e + \varepsilon_r^f \qquad \qquad \varepsilon_t = \varepsilon_t^e + \varepsilon_t^f \qquad \qquad (1)$$

and in the crushed zone there is

$$\varepsilon_r = \varepsilon_r^e + \varepsilon_r^p \qquad \qquad \varepsilon_t = \varepsilon_t^e + \varepsilon_t^p \qquad \qquad (2)$$

where  $\varepsilon_{\tau}^{\epsilon}$ ,  $\varepsilon_{t}^{\epsilon}$  are the elastic strains,  $\varepsilon_{\tau}^{f}$ ,  $\varepsilon_{t}^{f}$  are the fracture strains,  $\varepsilon_{\tau}^{p}$ ,  $\varepsilon_{t}^{p}$  are the plastic strains. It is assumed that in the crushed zone the material behaves like a granular isotropic medium, of specified residual cohesion C and the angle of internal friction  $\varphi$ . The equilibrium equations are

$$\frac{\partial \sigma_r}{\partial r} + \frac{\sigma_r - \sigma_t}{r} = 0 \tag{3}$$

and strain-displacement relations take the form

$$\varepsilon_r = \frac{\partial u}{\partial r} \qquad \varepsilon_t = \frac{u}{r}$$
(4)

The Hookes law for an isotropic material now provides

$$\varepsilon_{r}^{\epsilon} = \frac{1+\nu}{E} \left( (1-\nu)\sigma_{r} - \nu\sigma_{t} \right)$$

$$\varepsilon_{t}^{\epsilon} = \frac{1+\nu}{E} \left( (1-\nu)\sigma_{t} - \nu\sigma_{r} \right)$$
(5)

In the cracked zone, there is

$$\varepsilon_t^I = 0 \qquad \sigma_t = 0 \tag{6}$$

Assume the cracked zone to contain many cracks propagating from the internal boundary r=a to the interface boundary  $r=r_e$ . Using the Griffith condition of crack propagation, the potential energy release calculated at the progressing interface  $r=r_e$  is assumed to be equal stress intensity (or fracture toughness) of n cracks, so that

$$nK_{Ic}^2 = \pi r_e \left[ \left[ \sigma_t^2(r_e) \right] \right] \tag{7}$$

where the bracket |[]| denotes the discontinuity at  $r = r_e$ ,  $[\sigma_t^2(r_e)] = \sigma_t^2(r_e^+) - \sigma_t^2(r_e^-)$ .

The crushed zone follows the cracked zone for increasing internal pressure and the material satisfies the Coulomb yield condition

$$F_1 = \sigma_t - \sigma_r + (\sigma_r + \sigma_t) \sin \varphi - 2C_0 \cos \varphi = 0$$

$$F_2 = \sigma_r - \sigma_t + (\sigma_r + \sigma_t) \sin \varphi - 2C_0 \cos \varphi = 0$$

$$F_3 = \sigma_r - S_t = 0$$
(8)

 $F_4 = \sigma_t - S_t = 0$ 

where  $S_t$  denotes the tensile yield stress and  $C_0$  is the initial cohesion. Here  $F_1=0$ ,  $F_2=0$  represent the shear mode,  $F_3=0$ ,  $F_4=0$  correspond to tensile mode of flow. In the crushed zone it is usually assumed that the residual cohesion vanishes,  $C_r=0$ . The flow rule specifies the strain rates  $\dot{\varepsilon}_r^p$ , namely

$$\dot{\varepsilon}_{r}^{p} = \dot{\lambda} \frac{\partial g_{i}}{\partial \sigma_{r}}$$
 $\dot{\varepsilon}_{t}^{p} = \dot{\lambda} \frac{\partial g_{i}}{\partial \sigma_{r}}$ 
(9)

where  $\dot{\lambda} > 0$  and  $g_i$  is the plastic potential,

$$g_1 = \sigma_t - \sigma_r + (\sigma_r + \sigma_t)\sin\psi - 2C_g\cos\psi = 0$$

$$q_2 = \sigma_r - \sigma_t + (\sigma_r + \sigma_t)\sin\psi - 2C_g\cos\psi = 0$$
(10)

where  $\psi$  is the dilatancy angle and  $C_g$  is a constant. The potentials  $g_3 = 0$  and  $g_4 = 0$  are identical to  $F_3 = 0$ ,  $F_4 = 0$ .

#### 2.1 Solutions for specific zones

At the initial stage, the elastic zone occurs within the whole cylinder. The stress and strain distribution are governed by Lame equations and the critical pressure initiating cracking is

(5) 
$$p_{c} = S_{t} \frac{(b^{2} - a^{2})}{(b^{2} + a^{2})}$$
 (11)

where  $S_t$  is the characteristic tensile strength. The second phase corresponds to existence of two zones: elastic and cracked. In the elastic zone, the Lame solution applies with internal zone radius specifying the interface between cracked and elastic zones. The pressure acting on the interface is obtained from the solution for two zones and the crack propagation condition must be satisfied at  $r = r_c$ .

In the cracked zone we have

$$\sigma_r = \frac{A_1}{r} \qquad \sigma_t = 0$$

$$u = \frac{1 - \nu^2}{E} A_1 \ln r + A_2$$
(12)

where the integration constants follow from the radial stress and displacement continuity at  $r=r_f$ . Using the condition  $\sigma_r(r_f)=p$  and the cracking condition (7), the relation between the radius of cracked zone  $r_e$  and the pressure  $p_e$  acting at  $r=r_e$  is

$$p_e = K_I \sqrt{\frac{n}{\pi r_e} \frac{(b^2 - r_e^2)}{(b^2 + r_e^2)}} \tag{13}$$

Since at the onset of crack propagation there is  $r_e = a$ ,  $p_e = p_c$ , hence in view of (11) and (13), there is

$$S_t = K_I \sqrt{\frac{n}{\pi a}} \tag{14}$$

The internal pressure within the tube is now explicitly related to the size of the cracked zone, namely

$$p = S_t \sqrt{\frac{r_e}{a} \frac{(b^2 - r_e^2)}{(b^2 + r_e^2)}}$$
 (15)

The relation  $p(r_e)$  exhibits limit point at the critical crack length  $r_{ec}$  and the loading process is unstable for  $r_e > r_{ec}$ .

As in the cracked zone there is a uniaxial stress state  $\sigma_r \neq 0, \sigma_t = 0$ , the crushing starts when the pressure p exceeds the compressive strength  $S_c$ . Thus for  $p > S_c$ , the crushed zone propagates from the internal cylinder boundary.

The next stage corresponds to existence of crushed, cracked and elastic zones. At the interface between crushed and cracked zones there is  $p_f = S_c$  and for the radius  $r_e = r_{ec}$ , the radius  $r_f$  attains its maximum. The equilibrium evolution of states is achieved by assuming progression of cracked and crushed zones. The pressure acting at  $r = r_f$  now is

$$p_f = S_t \sqrt{\frac{r_e}{r_{fk}}} \frac{(b^2 - r_e^2)}{(b^2 + r_e^2)} \tag{16}$$

The details of further progression are discussed by Kowalczyk and Mróz (1988). Here, we only present the evolution of zones for

$$\frac{S_t}{E} = 0.001$$
  $\frac{C_0}{E} = 0.0012$   $\nu = 0.3$   $\varphi = \psi = 20^{\circ}$  (17)

In the case  $b/a = \infty$ , the progression of both cracked and crushed zones is stable and the respective diagrams are shown in Fig.2. Stability conditions for the case of progressing damage interfaces were considered by Dems and Mróz (1985).

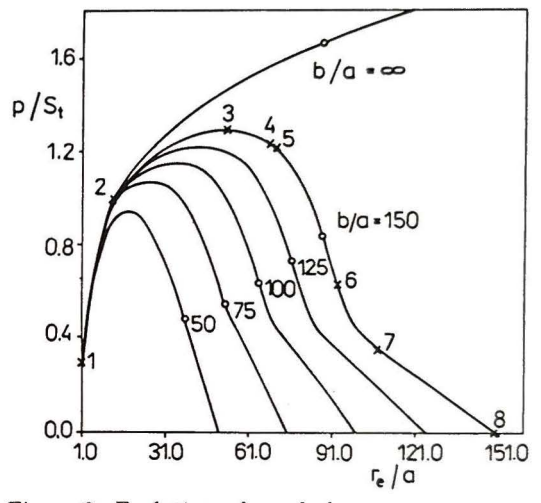


Figure 2: Evolution of cracked zone

### 3 PUNCH PENETRATION INTO PLASTIC-BRITTLE MATERIAL

The axisymmetric solution of the preceding section will now be used to construct a simplified solution of punch indentation in plane strain and plane stress cases. When a rigid punch is penetrated into an elastic semiplane, the stress concentration zones at punch edges induce localized cracking and crushing beneath the punch, cf. experimental data in papers by Pang et al (1989), (1990), Swain and Lawn (1976), Tokar (1990), Wagner and Schümann (1971), Wijk (1989), Lindqvist and Lai (1983). It is assumed that a crushed zone of radius  $r_f$  is formed with the hydrostatic stress state. This zone acts as a pressure loading on the remaining

material thus inducing cracking and subsequent shearing or buckling of the cracked material blocks. It is assumed that the cracked zone is bounded by a circle of radius  $r_e$  and radial lines  $\tau = \pm \alpha_I$ , Fig.3. The cracks are assumed to propagate along radial directions, so the axisymmetric solution can be assumed to predict the radius  $r_e$  of the cracked zone. For simplicity, we neglect the progressive crushing and growth of the initial crushed zone of radius r<sub>1</sub>. The subsequent failure mode within the plane develops in a form of localized shearing along velocity discontinuity lines, inducing motion of material toward the free surface. For an elasticplastic material the stage of development of localized shear bands should be considered. However, we assume that the failure mechanism develops instantaneously similarly as in rigid-plastic materials. On the other hand, in-plane stress state, the cracked beams are assumed to buckle in the outof-plane mode and subsequently they deform in a post-buckling stage until total failure of beams occurs due to bending fracture of end cross-sections. The post-critical stage is analysed by assuming

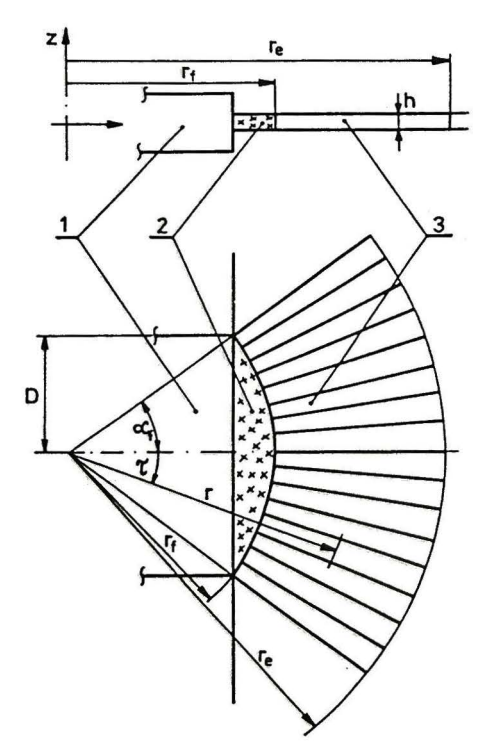


Figure 3: Simplified punch indentation model: 1) punch 2) crushed zone 3) cracked zone

the beams to be rigid with end cross-sections connected to the foundation by nonlinear springs of specified characteristics. These simplified assumptions are introduced in order to generate the analytical solution before more accurate incremental analysis will be provided.

#### 3.1 Progression of cracking zone

Assuming the crushed zone to be fixed and specified by the radius  $r_f = a$ , the axisymmetric solution will be applied setting  $b \to \infty$ . The cracking condition now is assumed in the form

$$\sigma_t(r_e) = S_t \left(\frac{r_f}{r_e}\right)^{\kappa} = S_t \left(\frac{a}{r_e}\right)^{\kappa} \tag{18}$$

where  $\kappa$  is a positive exponent. For  $\kappa=0$  we obtain the strength condition and for  $\kappa=\frac{1}{2}$  the energy condition. By selecting proper value of  $\kappa$ , one can account for the fact that now cracking develops within an annular segment of unspecified angle  $\alpha_f$  and number of cracks. The constants  $A_1$  and  $A_2$  occurring in (12) are now obtained from displacement and radial stress continuity conditions, so that

$$A_{1} = -S_{t}r_{e} \left(\frac{r_{f}}{r_{e}}\right)^{\kappa}$$

$$A_{2} = \frac{1+\nu}{E}S_{t}r_{e} \left(\frac{r_{f}}{r_{e}}\right)^{\kappa} \left[1+(1-\nu)\ln(r_{e})\right]$$
(19)

The pressure  $p_e$  is calculated from (18). Since  $p_f = -\sigma_r(r_f)$  the pressure in the crushed zone beneath the punch is

$$p_f = S_t \left(\frac{r_f}{r_e}\right)^{\kappa - 1} \tag{20}$$

For  $0 < \kappa < 1$ , the growth of the fracture zone requires monotonic growth of punch pressure. Hence for some value  $r = r_{ec}$ , a new failure mode is to develop within the fractured zone.

#### 3.2 Shear failure (plane strain case)

The second failure mode is assumed in a form of limit failure mechanism developed both in cracked zone and undamaged zones, typical for limit analysis, Fig.4. The shear planes  $A_0A_1$ ,  $A_0A_2$ ,  $A_1A_2$  and  $A_2A_3$  constitute kinematically admissible failure mechanism. However  $A_0A_1$ ,  $A_0A_2$ ,  $A_1A_2$  are passed through the cracked zone of reduced cohesion. On the other hand,  $A_2A_3$  passes through the undamaged material so the initial cohesion and

angle of friction should be used in calculating the dissipation rate. The balance of rate work and internal dissipation now is, cf. Mróz and Drescher (1968)

$$2DpV_0 = 2Cl_2V_2\cos\varphi \tag{21}$$

where D is the punch half-width,  $l_2$  denotes the length of the discontinuity line  $A_2A_3$ ,  $V_0$  is the punch velocity and  $V_2$  is the velocity of block  $A_1A_2A_3$ . In writing (21) we neglect the residual cohesion on  $A_0A_2$   $A_2A_1$  and  $A_0A_1$  assuming it to be much smaller then  $C_0$ . Using hodograph and geometric relations, we obtain

$$p = C_0 \left( \frac{u_f}{D} + \frac{\sin \alpha_1 \cos \alpha_f}{\cos \alpha_0 \cos(\alpha_0 - \alpha_1 - \alpha_f)} \right) \frac{\cos(\alpha_0 - \varphi) \cos(\alpha_0 - \alpha_1 - \alpha_f + 2\varphi) \cos \varphi}{\sin(\alpha_1 - 2\varphi) \sin(\alpha_2 - 2\varphi) \cos(\alpha_2 - \alpha_f)}$$
(22)

where the angles  $\alpha_0$ ,  $\alpha_1$ ,  $\alpha_2$  and the displacement  $u_f = u(r_f)$  are shown in Fig.4. The critical pressure is obtained by determining the minimum of  $p(\alpha_0, \alpha_1, \alpha_2)$ .

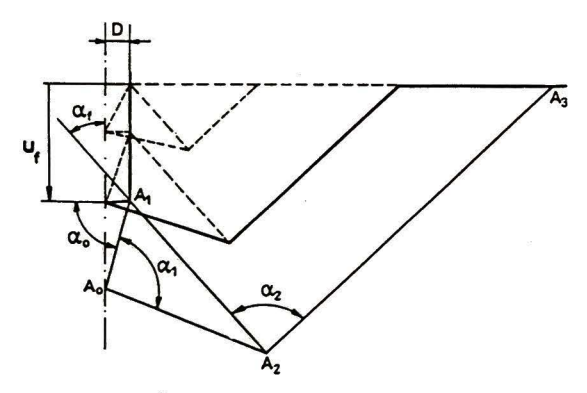


Figure 4: Kinematically admissible failure mechanism (third cycle in plane strain case)

#### 3.3 Buckling failure (plane stress case)

In the case of plate thickness h small with respect to punch width 2D, the plane stress condition prevails and the cracked material can be regarded as a set of tapered beams supported at  $r = r_e$ . The out-of-plane buckling mode of beams is therefore considered. The post-buckling response induces localized cracking and softening at  $r = r_e$ , which involve decreasing load acting on the beam.

Denoting  $k = r_f/r_e$ , and introducing the plane

stress elastic constants  $\nu_n = \nu/(1+\nu)$ ,  $E_n = E(1+2\nu)/(1+\nu)^2$ , we obtain the punch displacement and pressure in the form

$$u_f = \frac{S_t r_f}{E_n \sqrt{k}} [(1 + \nu) - \ln(k)] \qquad p_f = \frac{S_t}{\sqrt{k}}$$
 (23)

Denote by  $b_e$  and  $b_f$  the widths of cracked beams at  $r = r_e$  and  $r = r_f$ , by  $F = p_f h b_f$  the force acting on beam of length  $l = r_e - r_f$ . Depending on geometric parameters the buckling mode can occur within the plane or out-of-plane. The corresponding critical taper ratios are denoted by  $k_t$  and  $k_z$ . The following relations specify  $k_t$  and  $k_z$  at buckling

$$\frac{b_e(k_t)}{48l^2(k_t)}\theta_t(k_t)E_nh^3 - p_f(k_t)hb_f = 0$$

$$\frac{b_e(k_z)}{48l^2(k_z)}\theta_z(k_z)E_nh^3 - p_f(k_z)hb_f = 0$$
(24)

where  $\theta_t$  and  $\theta_z$  denote the buckling coefficients provided by Życzkowski (1956) in the tabular form. It follows from (23) that the critical taper ratio  $k_c$  and buckling mode are determined by the condition  $k_c = \max(k_t, k_z)$ . The values of  $b_e$  and  $b_f$  are

$$b_e = \frac{b_f}{k} \qquad b_f = \frac{2}{n-1} \alpha_f r_f \qquad (25)$$

where n denotes the number of cracks and  $\alpha_f = \arccos(D/r_f)$  is the opening angle of the cracked zone.

The post-buckling analysis is carried out by assuming the buckled bar as rigid with the inelastic hinge support at  $r=r_e$ . The bending moment  $M_g$  at the hinge depends on the rotation angle  $\vartheta$  according to the relations

$$M_{g}(\theta) = \begin{cases} C_{\theta}\theta & \text{if } \theta \leq \theta_{0} \\ C_{\theta}\theta_{0} - C_{1}(\theta - \theta_{0}) & \text{if } \theta_{0} < \theta \leq \theta_{1} \\ 0 & \text{if } \theta_{1} < \theta \end{cases}$$
(26)

where  $\vartheta_0$  and  $\vartheta_1$  denote critical values of  $\vartheta$  indicating the onset and termination of the hinge failure process. Here  $C_0$  denotes the hinge stiffness in the elastic stage and  $C_1$  is the postcritical softening modulus. The value of  $C_0$  is obtained from the value of the critical buckling load,  $C_0 = F(k_c)l(k_c)$ . The value of  $\vartheta_0$  is obtained by assessing the rupture stress of material fibers in tension, so that

$$S_t = -6 \frac{F(k_c)l(k_c)\vartheta_0}{b_c h^2} \tag{27}$$

where compressive stress was neglected. The value of  $\vartheta_0$  evaluated for ice is of the order  $10^{-5}$ . Higher values can be obtained by accounting for the compressive stress, thus

$$S_{t} = -\frac{F(k_{c})}{b_{c}h^{2}}\vartheta_{0}[hetg\vartheta_{0} + 6l(k_{c})]$$
(28)

The value of  $\vartheta_1$  corresponds to  $M_g(\vartheta_1) = 0$ . The punch displacement and stress vary in the post-critical stage according to the relations

$$u_f = \frac{S_t r_f}{E_n \sqrt{k}} [(1+\nu) - \ln(k_c)] + l(k_c)(1-\cos\vartheta)$$

$$p_f = \frac{M_g(\vartheta)}{l(k_c)h b_f \sin\vartheta}$$
(29)

When  $\vartheta = \frac{1}{2}\pi$ , the consecutive loading cycle commences and the periodic sequence of cracking, buckling, post-buckling modes develops.

#### 3.4 Discussion of theoretical solutions

For numerical analysis, the following parameters were assumed

$$S_t = 0.7MPa$$
  $S_c = 5MPa$  
$$E = 10GPa$$
  $\nu = 0.3$   $\varphi = 20^{\circ}$  (30)

typical for ice, cf. Sunder and Connor (1984). The problem parameters are D, h, n,  $\alpha_f$  and  $C_1$ . The

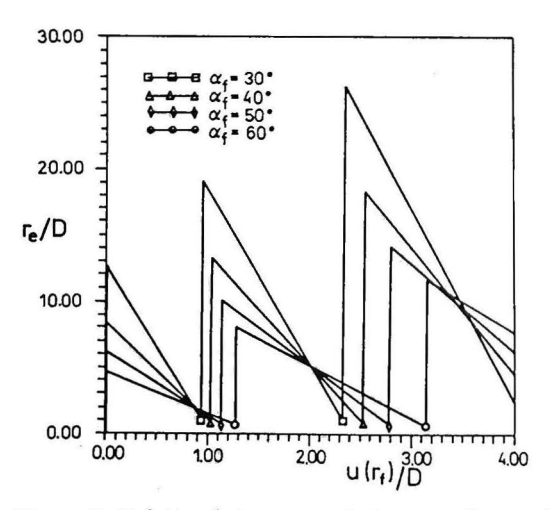


Figure 5: Relation between cracked zone radius and punch penetration depth (plane strain case)

experimental data indicate that for brittle materials the critical stress for punch indentation is of the order of  $p_c/S_c = 4\text{--}10$ , cf. Wijk (1989), and the cracked zone radius reaches the values  $r_e/D = 2\text{--}8$ , cf. Pang et al (1990). For the plane strain case, the cracked zone and punch pressure evolution are shown in Fig.5-6 as functions of punch displacements  $u_f/D$  for different values of the angle  $\alpha_f$  of cracked zone (assumed  $\kappa = 0$ ). It is seen that the predicted values are within the range of experimental observation. For specified values of  $\alpha_f$ .

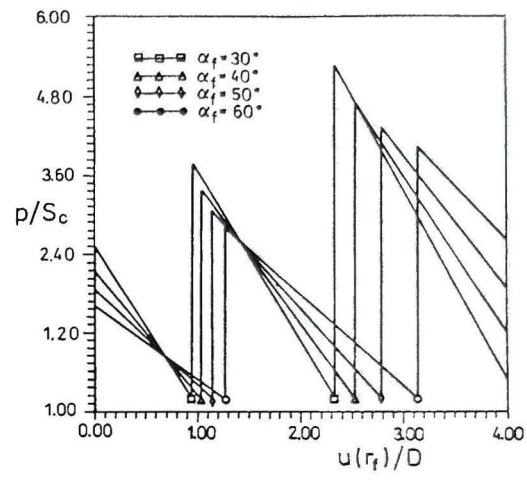


Figure 6: Relation between punch pressure and punch penetration depth (plane strain case)

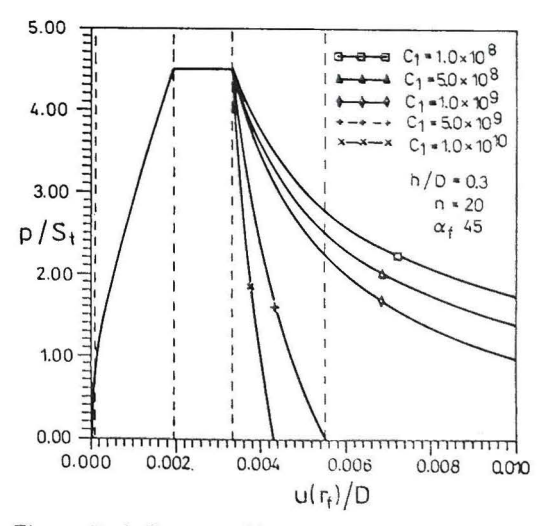


Figure 7: Influence of hinge softening stiffness on relation between punch pressure and punch penetration depth (plane stress case)

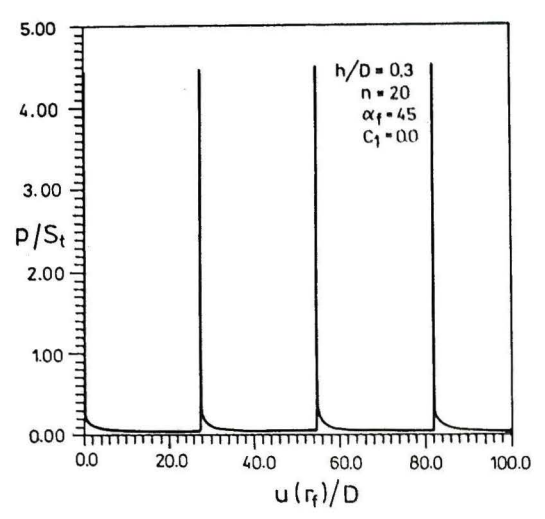


Figure 8: Relation between punch pressure and punch penetration depth (plane stress case)

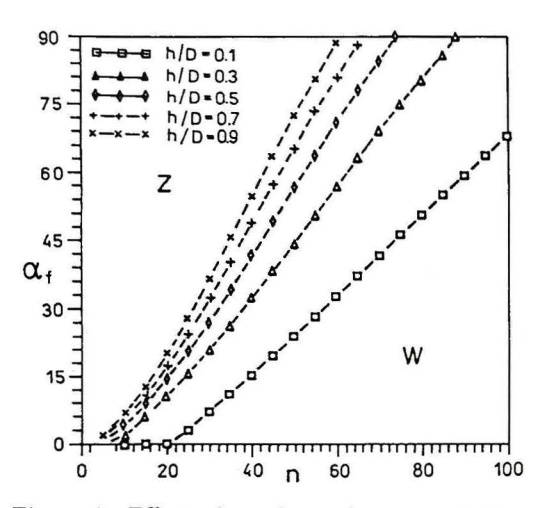


Figure 9: Effect of crack number on variation of buckling mode

the growth of cracked zone and maximal pressure is due to growth of the length of shear band in the final failure mode. Figures 7–8 show the respective curves for the plane stress case. The experiments carried for ice plates indicate that the maximal stress is reached at small punch displacements with subsequent drastic reduction of pressure for progressive punch penetration, cf. Michel and Toussaint (1977). The same character of load-displacement diagram was predicted by the present model. The effect of crack number on variation of buckling mode from in-plane to out-of-plane is il-

lustrated in Fig.9. Here the plot of lines  $k_t = k_z$  are shown with in-plane buckling (W) occurring below the curve and out-of-plane buckling occurring above the curve (Z). The effect of buckling mode leads to a new idea of damage mechanism in brittle materials. The buckling of cracked material was also considered by Bažant et al (1993).

#### 4. CONCLUDING REMARKS

The present analysis provides the insight into the progression of failure modes in brittle materials. These are termed as cracking, crushing, buckling, post-buckling and shearing modes. The analysis of consecutive modes and of their interaction provides the resulting force-displacement diagram, usually of oscillating character, indicating periodicity of mode evolution. The qualitative assessment provides results confirmed by experimental data and observation. A more refined analysis is needed predicting number of cracks and their evolution. However such analysis would be much more complex.

#### REFERENCES

- Z. P. Bažant, F. B. Lin, H.Lippmann, 1993, "Fracture Energy Release and Size Effect in Borehole Breakout.", Int. J. Numerical & Analytical Methods in Geomechanics, Vol. 17, No 1.
- N. G. W. Cook, M. Hood, F. Tsai, 1984, "Observations of Crack Growth in Hard Rock Loaded by an Indenter.", Int. J. Rock Mech. Min. Sci. & Geomech. Abstr., Vol. 21, No. 2, p.97-107.
- K. Dems, Z. Mróz, 1985, "Stability Conditions for Brittle-Plastic Structures with Propagating Damage Surfaces.", J. Struct. Mech., Vol. 13, No. 95.
- W. Derski, R. Izbicki, I. Kisiel, Z. Mróz, 1989, "Rock and Soil Mechanics", Elsevier.
- R. T. Ewy, N. G. Cook, 1990, "Cylindrical Opening in Rock.", Int. J. Rock Mech. Min. Sci. & Geomech. Abstr., Vol. 27, No. 5.
- K. Hellan, 1984, "An Asymptotic Study of Slow Radial Cracking.", Int. J. Fracture, Vol. 26, p.17-30.

- J. C. Jaeger, N. G. W. Cook, 1976, "Fundamentals of Rock Mechanics.", John Wiley & Sons, New York.
- M. Kowalczyk, Z. Mróz, 1988, "Analysis of the cracking and crushing mechanism around the opening in brittle materials", (in Polish), Archives of Mining Sciences, Vol. 33, No. 4, p.403-439.
- B. Ladanyi, 1967, "Expansion of Cavities in Brittle Media.", Int. J. Rock Mech. Min. Sci., Vol. 4, p.301-328.
- P. Lindqvist, Lai Hai-Hui, 1983, "Behaviour of the Crushed Zone in Rock Indentation.", Rock Mech. Rock Engng., Vol. 16, p.199-207.
- B. Michel, N. Toussaint, 1977, "Mechanisms and Theory of Indentation of Ice Plates.", J. Glaciology, Vol. 19, No. 81, p.285-300.
- Z. Mróz, A. Drescher, 1968, "Limit Plasticity Approach to Some Cases of Flow of Bulk Solids.", Transactions of the ASME, p.1-8.
- S. S. Pang, W. Goldsmith, M. Hood, 1989, "A Force-Indentation Model for Brittle Rocks.", *Rock Mech. and Rock Engng.*, Vol. 22, p.127-148.
- S. S. Pang, W. Goldsmith, 1990, "Investigation of Crack Formation During Loading of Brittle Rock.", Rock Mech. and Rock Engng., Vol. 23, p.53-63.
- S. S. Sunder, J. J. Connor, 1984, "Numerical Modeling of Ice-Structure Interaction", MIT Report.
- M. V. Swain, B. R. Lawn, 1976, "Indentation Fracture in Brittle Rocks and Glasses.", Int. J. Rock. Mech. Min. Sci. & Geomech. Abstr., Vol. 13, p.311-319.
- G. Tokar, 1990, "Experimental Analysis of the Elasto-Plastic Zone Surrounding a Borehole in a Specimen of Rock-Like Material Under Multiaxial Pressure.", Engng. Fracture Mechanics, Vol. 35, No. 4-5, p.879-887.
- H. Wagner, E. H. R. Schümann, 1971, "The Stamp-Load Bearing Strength of Rock an Experimental and Theoretical Investigation", Rock Mechanics, Vol. 3, p.185-207.

- G. Wijk, 1989, "The Stamp Test for Rock Drillability Classification.", Int. J. Rock Mech. Min. Sci. & Geomech. Abstr., Vol. 26, No. 1, p.37-44.
- M. Życzkowski, 1956, "Calculation of critical forces for elastic tapered beams", (in Polish), Rozpr. Inż., Tom IV, Zeszyt 3, p.367-412.